Article

Analysis of the Sound Field Structure in the Cabin of the RRJ-95NEW-100 Prototype Aircraft

Vladimir Lavrov [1], Petr Moshkov [2] and Dmitry Strelets [2,*]

1 IRKUT Corporation Regional Aircraft, Moscow 115280, Russia
2 Moscow Aviation Institute (National Research University), Moscow 125993, Russia
* Correspondence: dstrel@mai.ru or maksmai33@gmail.com

Abstract: The results of in-flight experiments to determine the structure of the sound field in the cabin and pressure fluctuation fields on the surface of the fuselage of the RRJ-95NEW-100 prototype aircraft are presented here. Wall pressure fluctuation spectrums are obtained for three zones of measuring windows (forward, center, and rear fuselage) in cruising flight mode. The effect of the jet on the pressure fluctuation levels in the tail fuselage is considered. For an aircraft without an interior, the contribution of the main sources to the total intensity calculated through A-weighted overall sound pressure levels is determined. It has been determined that the main noise sources in the cabin of the RRJ-95NEW-100 prototype aircraft in cruising flight mode are pressure fluctuation fields on the fuselage surface (turbulent boundary layer noise) and the air conditioning system. The ratio between the sources varies along the length of the cabin.

Keywords: aircraft; pressure fluctuations; cabin noise; RRJ-96NEW-100; aeroacoustics

1. Introduction

The development of civil aircraft construction is closely related to the issues of reducing community noise and improving the acoustic comfort of passengers and crew members. In contrast to the topic of community noise, where noise levels are regulated by the ICAO standard [1], there are currently no international standards regulating the maximum permissible noise levels in aircraft cabins. In Russia, there is a national standard GOST 20296-2014 [2], which regulates the maximum permissible noise levels in the cabins of airplanes and helicopters. Noise measurements in the cabins are carried out in accordance with ISO 5129:2001 [3].

Currently, Russia is developing a joint standard GOSR R 70066–2022 "Aircraft equipment. Requirements for aircraft acoustic design of passenger salon and crew cockpit" [4]. Under these standards, the main research and development (R&D) methods are formulated, the performance of which at different stages of the aircraft design, it is necessary to ensure, meet the required parameters of acoustic comfort. The effective date of the standard in Russia is 1 March 2023.

A separate place in the problem of providing acoustic comfort is occupied by business aviation. In this class of aircraft, while providing relatively low noise levels of 65–70 dBA in the cabin, new problems arise related to human perception of noise. It is known that with the same overall sound pressure levels in the cabin in the dBA metric, cabin noise is perceived differently [5–7]. In addition, there is a need to assess the sound quality and ensure the required acoustic characteristics of the cabin in a way that is not related to the dBA metric.

In Russia, the RRJ-95NEW-100 aircraft is currently being designed on the basis of the Superjet 100 aircraft, taking into account the requirements of maximum import substitution of components and systems, including the replacement of the SaM-146 engine with the promising PD-8. The presented work was carried out as part of the implementation of a

complex of R&D aimed at providing the concept of acoustic design of the RRJ-95NEW-100 aircraft [8] in order to meet competitive market requirements, including the parameters of acoustic comfort of aircraft in the business jet segment.

The work is carried out as part of R&D on the design of the RRJ-95NEW-100, taking into account the requirements of increased acoustic comfort of passengers and crew members relative to the prototype aircraft Superjet 100. Within the framework of the presented work, the following tasks are solved:

(1) Determination of the structure of wall pressure fluctuation fields on the fuselage of the Superjet 100 prototype aircraft RRJ-95 NEW-100 in cruise flight mode. Obtaining information for the identification of noise sources in the cabin, as well as initial data for numerical simulation of turbulent boundary layer noise.
(2) Study of the sound field structure in the cabin of an airplane without an interior. Identification and ranking by intensity of the main noise sources.

2. Noise Sources in the Cabin of an Aircraft with a Classic Configuration of the Power Plant

The main sources of noise in the cabin of an aircraft with a configuration of turbofan engines on pylons under the wing are:

- Wall pressure fluctuation fields in the turbulent boundary layer (TBL) on the fuselage surface of the aircraft, leading to fluctuations in the skin and noise emission into the cabin. This source is usually called the turbulent boundary layer noise [9,10].
- Acoustic radiation of the power plant [11,12].
- The vibration effect of engines [13], which leads to the emission of so-called structural-borne noise into the cabin at characteristic rotary frequencies.
- Internal systems and equipment of the aircraft. Firstly, the air conditioning system (ACS) [14]. However, when designing an aircraft, the possible influence of other systems and noise-making equipment in the cabin should be taken into account [15].

The design mode for assessing the cabin noise and optimizing the design and systems of the aircraft in terms of noise minimization is the level of cruise flight. Special experiments are performed to separate noise sources and determine their relative contribution. In particular, it is possible to determine the contribution of the jet in the rear fuselage of the cabin by comparative analysis of noise measurements in the cabin in cruising flight mode and during the descent, with cruising speed in the idle power mode with a small pitch angle of aircraft. To determine the contribution of ACS, it is briefly turned off in flight. At the same time, disabling the ACS on an experimental aircraft implies cutting off the air supply to the cabin. The fans that are part of the system and the ACS cooling components continue to work at the same time.

3. Test Procedure and Processing of Measurement Data

3.1. Determination of the Structure of Pressure Fluctuation Fields on the Fuselage Surface

The tests were carried out on a Superjet 100 aircraft with the serial No. 95003. The general view of the aircraft, as well as the layout of the transducers within one measuring window, are shown in Figure 1a.

During the tests, the 15 relative pressure transducers of type Kulite XCS-190M-15D with a pressure range of 15 psi were installed in 3 measuring windows, each in 5 pieces as shown in Figure 1a. The numbers of the measuring windows, 2, 10, and 28, correspond to the locations of the windows on the aircraft. Additionally, 4 absolute pressure transducers of type Kulite LQ-2-500-25A with a pressure range of 25 psi were installed in the fuselage rear. The scheme of their placement is shown in Figure 1b.

When installing the transducers in the measuring windows, the deviation of the transducer plane from the plane of the measuring windows was not more than 20 microns. The ledge (deepening) of the measuring window relative to the fuselage corresponds to the real window of the Superjet 100. Absolute pressure transducers in the rear fuselage were

installed in special fairings. Unfortunately, the absolute pressure sensor No. 1 (Figure 1b) was damaged and registered an incorrect signal.

(a)

(b)

Figure 1. General view of the Superjet 100 No. 95003 with installed measuring windows in the forward (No. 2), central (No. 10), and rear (No. 28) parts of the fuselage on the left side (**a**) and 4 absolute pressure transducers installed in the fuselage rear (**b**).

Within the framework of this work, based on the results of complex flight tests, 2 flight modes were considered to determine the structure of pressure fluctuation fields in cruising flight mode and the influence of the acoustic field of the jet on the pressure fluctuation levels in the rear fuselage:

(1)   M = 0.78, FL 360 (M—flight Mach number; FL—flight level, 100 ft) cruising mode at the engine speed in percent of nominal (N1) 90%;

(2)   M = 0.78 FL 295 . . . 360. Idle engine mode (N1 = 58%). Descent from FL 360 at a constant airspeed.

Mode 1 is a level cruising flight mode. Mode 2 is a flight at cruising speed when the engines are switched to idle power mode while the pitch angle decreases slightly, and the aircraft begins to descent during the recording of the signal from FL 360 to FL 295.

In total, 2 flights were performed within the framework of this test program. Each mode in each flight was recorded 3 times for 60 s. Pressure signals were recorded in parallel with all measuring channels to the on-board measurement system of the aircraft with a sampling frequency of 8192 Hz.

3.2. Measurements of Noise Levels in the Cabin of an Aircraft without an Interior

Tests to study the sound field structure in the cabin of the RRJ-95NEW-100 prototype aircraft were performed on the Superjet 100 aircraft with the serial No. 95157. The interior of the passenger cabin was dismantled on this aircraft, but the sound insulation materials were installed in full.

Within the framework of these flight tests, 3 flight modes and the operation of the ACS were considered to separate the main sources and determine their relative contribution along the length of the aircraft cabin:

1. M = 0.78, FL 360, ACS ON. Cruising flight mode during normal operation of the air conditioning system.
2. M = 0.78, FL 360, ACS OFF. Cruising flight mode when the air supply to the cabin is blocked.
3. M = 0.78, FL 295...360, ACS ON, idle engine operation mode (N1 = 58%). Descent from the FL 360 at a constant airspeed.

The noise measurement control points were located on the right and left sides at a height of 1.2 m relative to the floor line and at a distance of 0.5 m from the side opposite the specified bulkheads.

Measurements were carried out on the right and left sides:

- In the front service area of bulkhead No. 12 (right side) and No. 13 (left side);
- In front of bulkhead No. 17 and 20;
- In the area of center of bulkhead No. 24, 27, and 31;
- In the rear part of the cabin bulkhead No. 35, 40, 43, and 46;
- In the rear service area of bulkhead No. 48.

Only 22 were considered as the reference points.

Sound signal measurements were performed for 40 s at each control point with a sampling frequency of 48 kHz. Further signal processing included, for the purposes of this work, obtaining 1/3-octave spectrum of sound pressure levels averaged over the recording time interval. All recorded and processed signals were quasi-stationary.

4. Structure of Pressure Fluctuation Fields on the Fuselage Surface

4.1. Spectrum of Pressure Fluctuation Levels in Cruising Flight Mode

Preliminary results are presented by the authors in Ref. [16]. The narrowband spectrum of pressure fluctuations with a bandwidth (Δf) of 8 Hz, measured within three measuring windows at five control points, are considered in Figure 2. The spectrum is broadband and two frequency ranges can be distinguished in them, characterized by different dependences of spectral level reduction with frequency. This is a range of 300–2000 Hz and a frequency range of 2000–3020 Hz. The indicator of the pressure fluctuation intensity decline curve for the frequency range 300–2000 Hz averages −0.9 for three measuring windows, and −8.3 for the frequency range 2000–3020 Hz. In the frequency range of 20–300 Hz, there is a slight increase in the measured levels of pressure fluctuations.

The forms of the pressure fluctuation spectrum are consistent with the results of studies by other authors [17–19] and semiempirical models, describing the Robertson [20]/Cockburn and Robertson models [21], respectively, and the Efimtsov 1 [22] and 2 [23]/Rackle and Weston models [24]. Furthermore, the absence of tonal components in the pressure fluctuation spectrum indicates the dominance of the pressure fluctuation field over the engine's acoustic radiation.

The spread of measured levels within the measuring window No. 2 is ≈5 dB. Within the measuring window No. 10 it is ≈10 dB. For the measuring window No. 28, the average level spread over the spectrum does not exceed 1 dB.
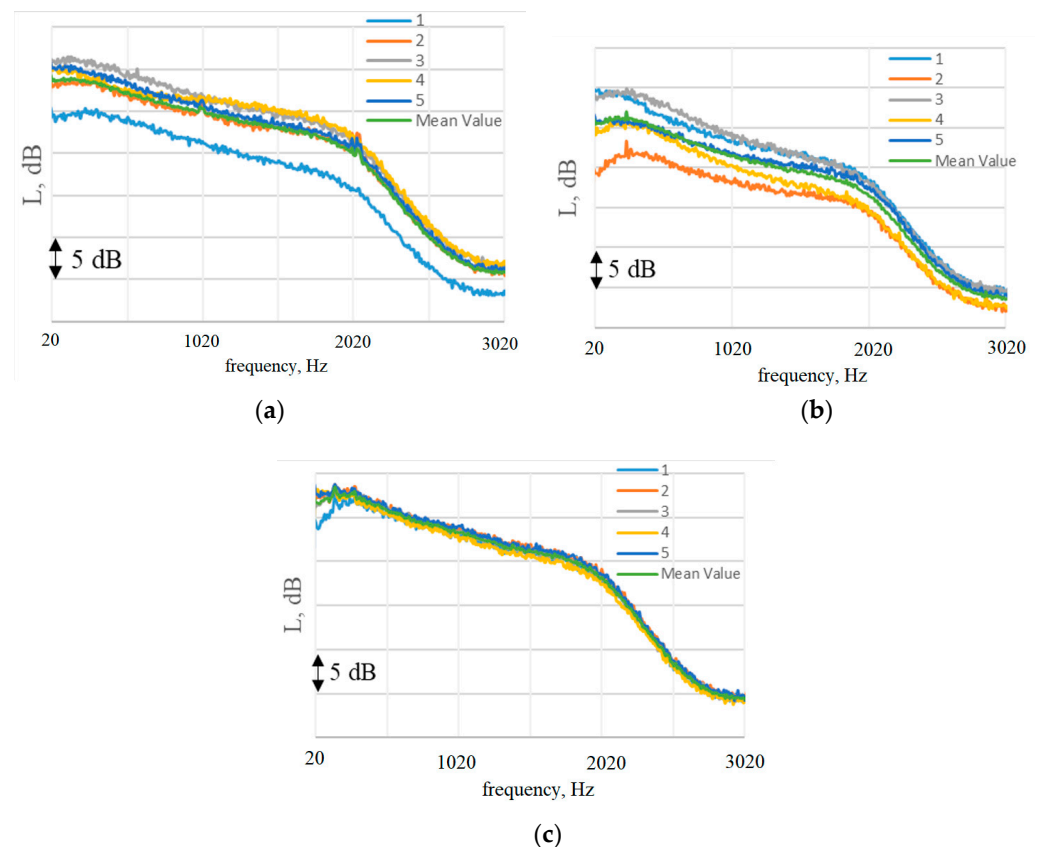
Figure 2. Narrowband pressure fluctuation spectrum measured at different control points within three measuring windows in cruise flight mode (M 0.78, Δf = 8 Hz). (**a**) Measuring window No 2. (forward fuselage). (**b**) Measuring window No. 10 (center fuselage). (**c**) Measuring window No. 28 (rear fuselage).

The blue curve on the graph (Figure 2a) corresponds to the measurements made by transducer No. 1 (Figure 2a), located above other sensors within measuring window No. 2. This pattern was observed when all measurements were performed in this measuring window. Checking the calibration of the transducer did not reveal violations that could, equidistant by 5 dB, underestimate the measured levels of pressure fluctuations relative to other transducers. If the sensor is not installed flush with respect to the plane of the measuring window, significant deviations in the measured levels up to a frequency of 500 Hz should be expected, without affecting the measured levels at high frequencies [24]. Thus, at this stage of the study, it is not possible to explain this effect.

The variation in the levels of pressure fluctuations measured in measuring window No. 10 (Figure 2b) is most likely due to the proximity of the measuring window to the wing nose.

At the same time, the location of the control point within measuring window No. 28 (Figure 2c), located in rear fuselage, does not actually affect the measured levels of pressure fluctuations.

4.2. The Effect of the Jet in the Fuselage Rear

The effect of the jet on the measured levels of pressure fluctuations is considered in Figure 3. There is a comparison of the measurement results in the measuring window No. 28 (rear fuselage) of narrowband spectrum averaged over five control points in cruising flight mode and when the aircraft is descending at the same airspeed (M 0.78) in idle engine operation mode (N1 = 58%) with a pitch angle of −4°.
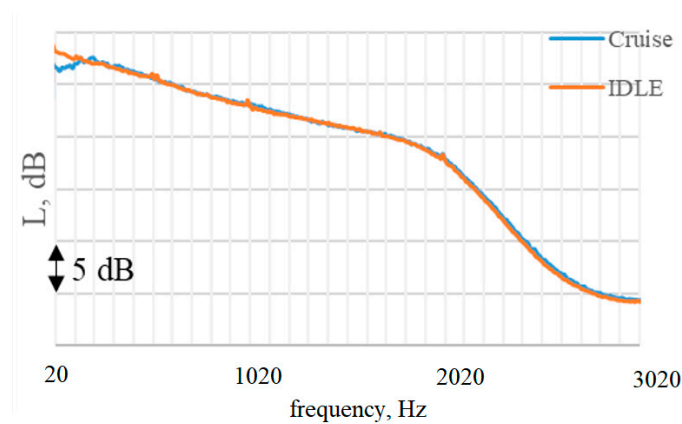
Figure 3. Comparison of narrowband pressure fluctuation spectrum averaged over five control points, measured in the measuring window No. 28 in cruising flight mode and descent mode when the engines are idle (M 0.78, Δf = 8 Hz).

It can be seen that the aeroacoustics effect of the jet in the area of the measuring window No. 28 is not observed in the entire studied frequency range.

A comparison of the pressure fluctuation spectrum recorded by absolute pressure transducers at control points No. 2–4 (Figure 1b) is considered in Figure 4. The greatest influence of the reduced power mode (idle) at constant airspeed is observed at control point No. 2, located closer to the engine nozzle at frequencies above 400 Hz. For control point No. 3, the effect of the jet is observed up to a frequency of 1500 Hz. At control point No. 4, at frequencies above 500 Hz, a slight increase in spectral levels is observed when the engine power mode is idle.

(**a**)

(**b**)

(**c**)
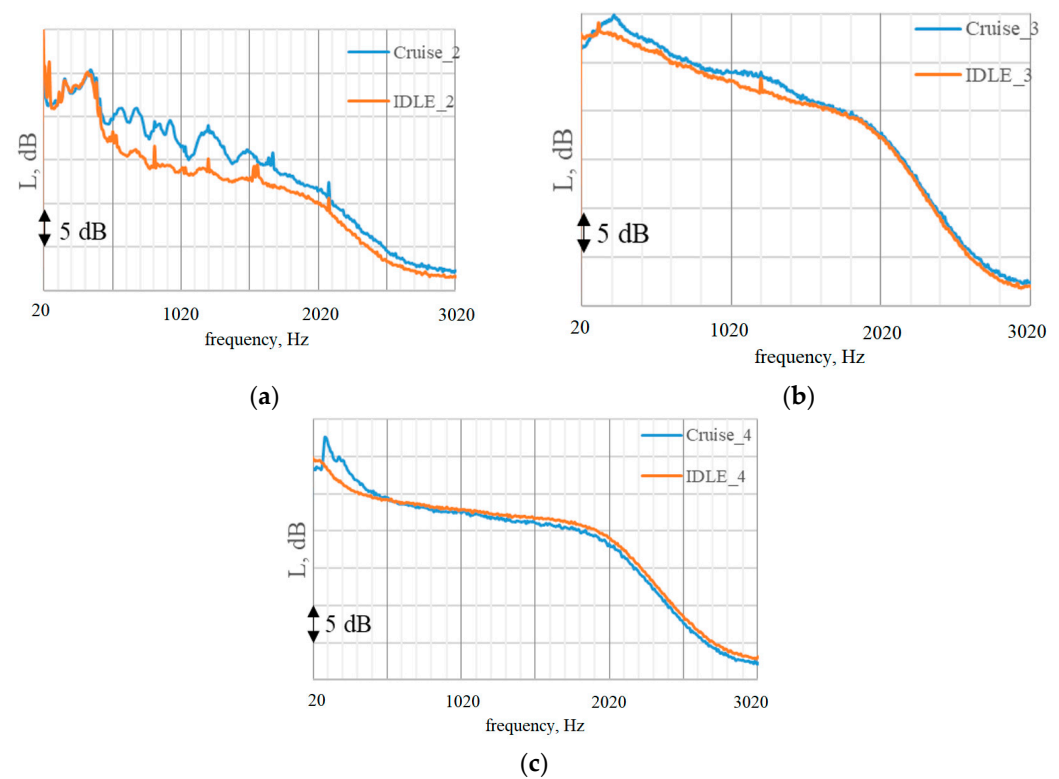
Figure 4. Comparison of narrowband pressure fluctuation spectrum measured at the control points No. 2–4 (Figure 1b) in cruising mode and descent mode when the engines are idle (M 0.78, Δf = 8 Hz). (**a**) No. 2. (**b**) No. 3. (**c**) No. 4.

Thus, within the framework of this experiment, taking into account the location of the pressure transducers, it can be concluded that the jet of the engine has an aeroacoustics effect on the fuselage at the control point No. 2, closest to the nozzle section and located below the floor line. At other control points, the aeroacoustics effects of the jet are insignificant.

5. The Structure of the Sound Field in the Cabin in Cruise Flight Mode

5.1. Spectral and Integral Characteristics of the Sound Field in the Cabin

The change in the A-weighted overall sound pressure levels along the length of the cabin on the right and left sides is considered in Figure 5. From 16 to 27 of the bulkheads, the sound pressure levels decrease slightly (by 2 dBA), and then increase to the tail by 5–6 dBA. In general, the deviation of the measured overall sound pressure levels from the right and left sides from the mean value does not exceed 0.5 dBA.
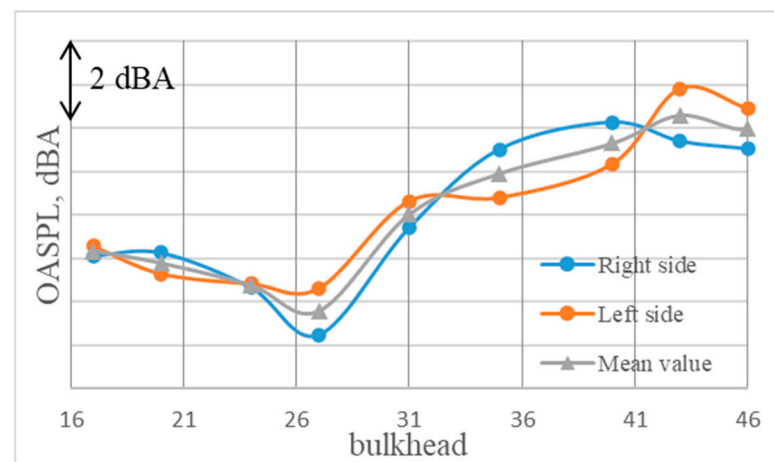
Figure 5. Change in the A-weighted overall sound pressure levels (25–10,000 Hz) along the length of the cabin on the right and left sides (M 0.78, ACS ON).

A comparison of the 1/3-octave spectrum of sound pressure levels measured at various control points along the length of the cabin on the right side is shown in Figure 6. It can be seen that when the control point is moved to the tail of the cabin, the spectrum of sound pressure levels is transformed. Sound pressure levels in the frequency range of 100–1000 Hz increase, and in the high frequency range of 1000–10,000 Hz decrease. The transformation of the spectra may indicate a change in the ratio of the main noise sources along the length of the cabin.
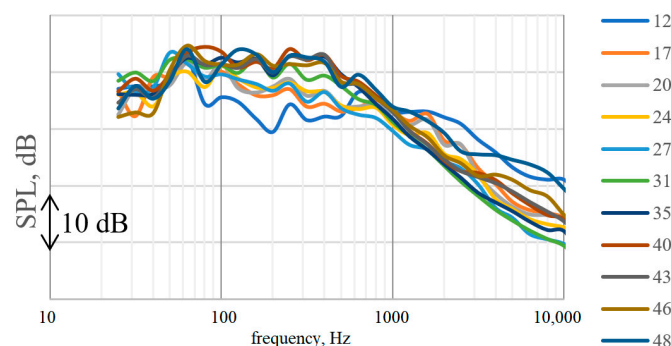
Figure 6. Comparison of 1/3-octave spectrums of sound pressure levels measured along the length of the cabin on the right side in the frequency range 25–10,000 Hz (M 0.78, ACS ON).

5.2. Influence of ACS Activity

The effect of the ACS switching off on the A-weighted overall sound pressure levels, measured from the left side, is considered in the Figure 7. The greatest effect when the ACS

is switched off is observed in the tail section of the cabin, in the zone from 43 to 48 of the bulkheads and is 2.5 dBA. In zone 35 of the bulkhead, there is an increase in the overall noise level by 1 dBA when the ACS switching off.
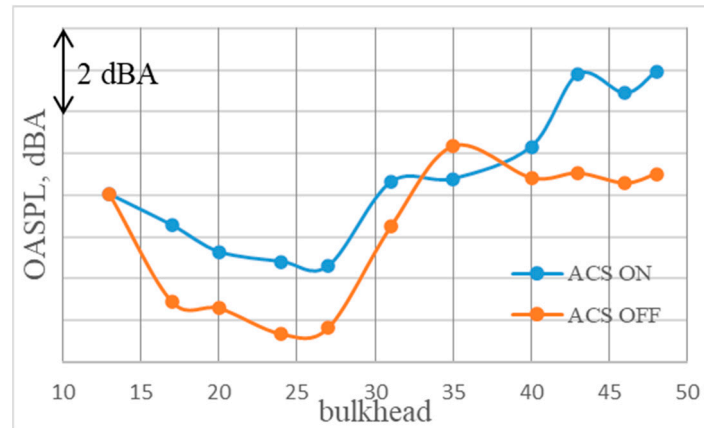
Figure 7. The effect of switching off the ACS on the A-weighted overall sound pressure levels measured from the left side (M 0.78).

The effect of the ACS operating mode on the 1/3-octave spectrum of sound pressure levels measured on the left side, in the area of bulkheads No. 35 and 43, is considered in Figure 8.

(**a**)

(**b**)
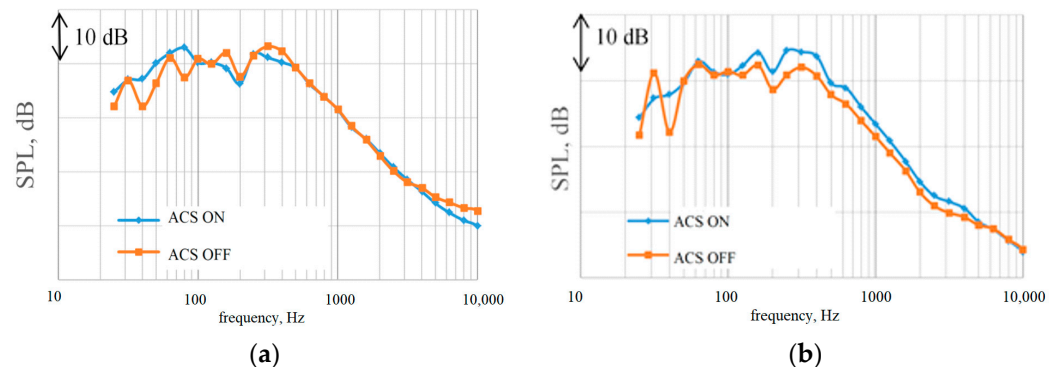
Figure 8. The effect of switching off the ACS on the 1/3-octave spectrum of sound pressure levels measured from the left side (M 0.78). (**a**) Bulkhead No. 35. (**b**) Bulkhead No. 43.

The increase in the overall noise level in bulkhead No.35 by 1 dBA (Figure 7) is due to an increase in sound pressure levels in the frequency range 125–500 Hz (Figure 8a). Since the fans in the system continue to work when the ACS is turned off, it can be assumed that the increase in sound pressure levels is most likely due to an increase in the noise of the ACS fans in the absence of an incoming flow. The fan speed of the system is 380 Hz, which corresponds to a 1/3-octave frequency band of 400 Hz. In addition, the previously performed experiment [25] made it possible to localize the sources of increased noise in the 400 Hz frequency band from the side of the air supply pipelines to the passenger cabin.

In the area of bulkhead No. 43 (Figure 8b), it can be seen that switching off the ACS leads to a decrease in sound pressure levels in the frequency range of 160–5000 Hz, which leads to a decrease in the A-weighted overall sound pressure level by 2.5 dBA.

5.3. Influence of Jet Noise

In order to determine the contribution of the acoustic radiation of the power plant, within the framework of these tests, a flight mode with a descent at a constant speed

(M 0.78) with a small pitch angle (−4°) from the FL 360 was considered when switching engines from cruising power mode (N1 = 90%) to idle (N1 = 58%).

The distribution of the A-weighted overall sound pressure levels, measured along the length of the cabin on the right side at the FL 360 and when descent in idle engine power mode (M = 0.78) is shown in Figure 9. The greatest decrease in the overall noise level of 2 dBA is observed on the right side in the zone of bulkhead No. 40.
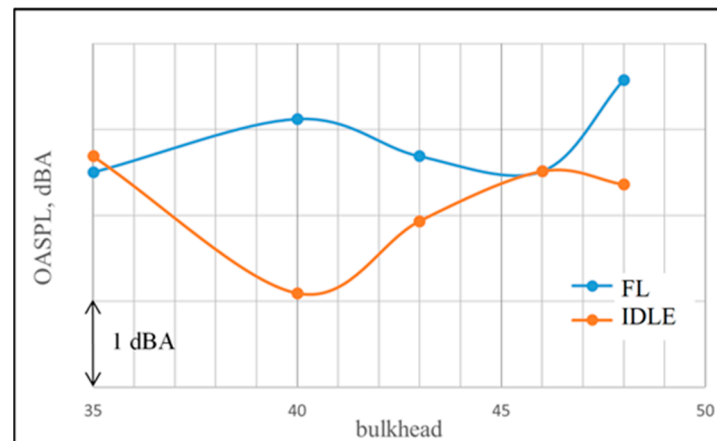
Figure 9. Distribution of the A-weighted overall sound pressure levels along the length of the tail section of the cabin on the right side at the FL 360 and during a descent in idle power mode (M = 0.78, ACS ON).

A comparison of the 1/3-octave spectrum of sound pressure levels measured on the right side at the FL 360; when descent during idle power mode in the zone of the greatest influence of the jet (bulkhead No. 40); and in the zone where no effect was detected (bulkhead No. 35) is considered in Figure 10a,b. Since when switching engines to idle power mode sound pressure levels at frequencies above 2000 Hz decrease significantly (Figure 10a), it can be concluded that jet noise dominates in the frequency range 2000–10,000 Hz. This result is consistent with the results of noise studies in the cabin of the Superjet 100 No. 95009 aircraft with a VIP interior [25], but in that study the effect of the jet was determined in the frequency range of 1600–10,000 Hz.

(a)   (b)
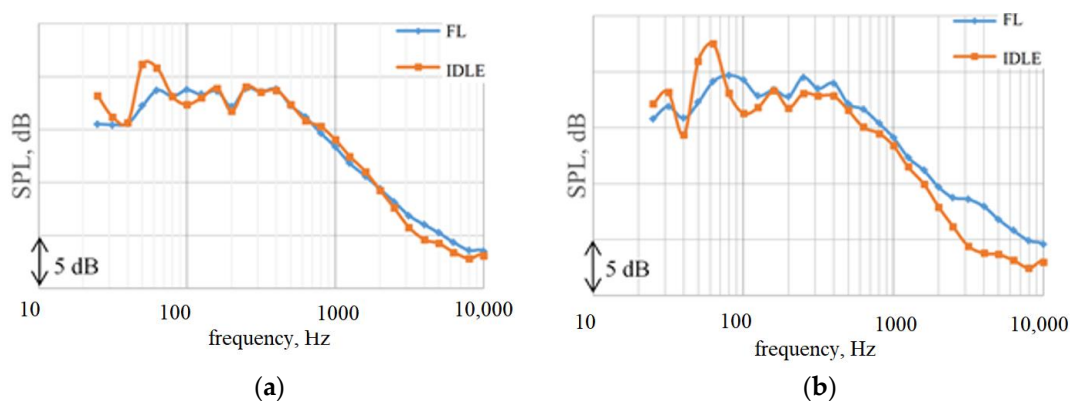
Figure 10. Comparison of 1/3-octave spectrums of sound pressure levels measured on the right side at the FL 360 and during a descent in the idle power mode (M = 0.78, ACS ON). (**a**) Bulkhead No. 35. (**b**) Bulkhead No. 40.

In the zone of bulkhead No. 40, when switching engines to idle power mode, the greatest effect is observed at frequencies above 2000 Hz. However, there is a slight decrease in sound pressure levels in the range of 1/3-octave frequency bands 80–1600 Hz. This effect is most likely related to the peculiarities of the ACS operation when taking air from the

engines when they are switched to idle power mode. This effect should be studied in more detail in further studies.

It should also be noted that when switching engines to idle power mode, the tonal component of structure-borne noise is shifted to the frequency band of 63 Hz, while its intensity level increases significantly.

5.4. Ranking by Intensity of the Main Noise Sources along the Length of the Cabin

When assessing the contribution of the main noise sources along the length of the cabin, the following assumptions were made:

- Due to the absence of prominent tonal components of engine fan noise over broadband radiation, it was assumed that the contribution of the engine fan to the overall sound field in the passenger cabin was insignificant. In general, the level of the first tone of fan noise for engines with a bypass ratio of 4–6 is 5–10 dB higher than the levels of the broadband component of fan noise. Therefore, the broadband component of the fan noise does not stand out against the background of the noise of the turbulent boundary layer.
- It was assumed that the sound pressure level in the 1/3-octave band frequency of 100 Hz, including the rotary frequency of the engine fan shaft (96 Hz), is determined by the structure-borne noise of the engine.
- To assess the contribution of the jet of the engine in the tail section of the cabin, it was assumed that the noise levels in the tail section of the cabin at frequencies above 2000 Hz are due to the jet noise. From 12 to 31 bulkheads, the jet contribution was not evaluated due to the expected insignificance of this source when considering the forward and central part of the fuselage.
- Due to the impossibility of turning off the fans and cooling components of the ACS, it was assumed that turning off the ACS on the aircraft leads to the shutdown of the noise source of the ACS, which can be called "turbulent flow noise" in the air ducts of the system. This component of ACS noise was estimated on the basis of energy subtraction:

$$SPL_{ACSTF} = 10 \log \left(10^{0.1 SPL_{ACSON}} - 10^{0.1 SPL_{ACSOFF}} \right),$$

where SPL_{ACSTF}—sound pressure level of turbulent flow noise of ACS; SPL_{ACSON}—sound pressure level when the ACS is turned on; SPL_{ACSOFF}—sound pressure level when the ACS is turned off.

Table 1 presents a calculated estimate of the contribution of different noise components to the total intensity calculated using the A-weighted overall sound pressure levels along the length of the cabin for the right side.

Table 1. Assessment of the contribution of the main noise sources in the cabin (in %) to the total intensity calculated through the A-weighted overall sound pressure levels along the length of the cabin on the right side.

Source/Bulkhead No.	12	17	20	24	27	31	35	40	43	46	48
Structure-Borne Noise	0.2	0.8	1.1	1.1	1.1	0.9	0.8	0.9	0.6	0.6	0.5
Jet Noise (Above 2000 Hz)	–	–	–	–	–	–	2.6	3.5	3.8	5.1	8.9
ACS (Turbulent Flow Noise)	20.5	30.2	40.6	32.6	23.3	25.1	33.4	9.9	12.3	33.9	42.3
TBL + ACS Fan Noise	79.3	69.0	58.4	66.2	75.6	74.0	63.2	85.7	83.4	60.4	48.3

In Table 1, several values are distinguished from the general trend. These are bulkheads No. 40 and 43, where the contribution of the noise component of the ACS (turbulent flow noise) turned out to be significantly less than at other control points along the length of the cabin. Nevertheless, the data presented in Table 1 indicate the dominance of the turbulent

boundary layer noise and the ACS noise when assessing the A-weighted overall noise level in the cabin.

At the same time, the previously noted transformation of the measured spectrum of sound pressure levels along the length of the cabin is reflected in the ratio between the main sources. The contribution of ACS (turbulent flow noise) to the rear fuselage increases, and the contribution of the turbulent boundary layer noise decreases, in part due to the addition of jet noise in the tail section of the cabin.

The presented results of determining the structure of pressure fluctuation fields are fully consistent with the previously performed study [16,26] and complement it in terms of determining the effect of the jet on the recorded levels of pressure fluctuations in the tail fuselage. The tonal components of engine noise do not stand out against the background of the broadband component of pressure fluctuation fields. The results of the author's research are consistent with the experiments of other authors [17–19,27].

The results of the assessment of the contribution of the main sources along the length of the cabin to the total intensity, calculated using A-weighted sound pressure levels, do not contradict previously performed studies on aircraft with a classic configuration of the power plant: two turbofan engines on pylons under the wing [28–31].

When measuring pressure pulsation fields with transducers located in the measuring window No. 28, it was not possible to detect the influence of a jet, i.e., the aeroacoustics effect of the jet in this fuselage zone. The noise of the jet in the cabin of the RRJ-95NEW-100 prototype aircraft appears to be transmitted by design from the lower part of the fuselage and has a decisive effect on the noise levels in the cabin at frequencies above 1600–2000 Hz in the 1/3-octave frequency bands, depending on the configuration and types of acoustic materials used. It can be stated that for the RRJ-95NEW-100 aircraft, it is impractical to reduce the jet noise at the source by using such reduction methods as chevrons [32–34], since the jet noise is insignificant when assessing the overall noise level in the cabin.

The effect of the jet observed in the flight experiment below the floor line indicates that for promising aircraft configurations with engines located above the wing [35–37], providing community noise reduction due to the shielding effect, from the point of view of cabin noise, the jet should play an essential role in the formation of the sound field in the cabin.

6. Conclusions

A complex of aeroacoustics experiments was performed on an experimental prototype aircraft (Superjet 100) of the projected RRJ-95NEW-100.

(1) The structure of the wall pressure fluctuation fields on the fuselage surface in cruise flight mode was determined, the effect of the engine jet on the pressure fluctuation levels in the tail section of fuselage was estimated.

(2) For an aircraft without an interior, a study of the sound field structure in the cabin was performed. The contribution of different sources to the total sound intensity along the length of the cabin, calculated through A-weighted overall sound pressure levels was determined. It is shown that the main noise sources in the cabin of the RRJ-95NEW-100 prototype aircraft are wall pressure fluctuation fields on the fuselage surface (TBL noise) and the air conditioning system. The contributions of jet noise and structure-borne noise from the vibration effects of engines do not seem significant when assessing the overall noise levels in the cabin in the dBA metric.

The ratio between noise sources determines the concept of acoustic design of the RRJ-95NEW-100 aircraft. Most attention is paid to the development of an optimal scheme for the placement of acoustic materials in the on-board structure and research aimed at reducing the noise of the elements of the air conditioning system.

Author Contributions: Conceptualization, V.L. and P.M.; methodology, P.M. and D.S.; formal analysis, P.M. and D.S.; investigation, V.L. and P.M.; writing—original draft preparation, V.L., P.M. and D.S. All authors have read and agreed to the published version of the manuscript.

Conflicts of Interest: The authors declare no conflict of interest.

References

1. Environmental Protection. *Annex 16 to the Convention on International Civil Aviation. Volume 1 Aircraft Noise*; ICAO: Montreal, QC, Canada, 2011.
2. *GOST 20296-2014*; Aircraft and Helicopter of Civil Aviation. Acceptable Noise Levels in Flight Decks and in Salons and Methods of Noise Measurement. Russian Technical Standard: Russia, 2014.
3. *ISO 5129:2001*; Acoustics. Measurement of Sound Pressure Levels in the Interior of Aircraft During Flight. ISO: Geneva, Switzerland, 2001.
4. *GOST R 70066–2022*; Aircraft equipment. Requirements for Aircraft Acoustic Design of Passenger Salon and Crew Cockpit. Russian Technical standard: Russia, 2022.
5. Genuit, K. The sound quality of vehicle interior noise: A challenge for the NVH-engineers. *Int. J. Veh. Noise Vib.* **2004**, *1*, 158–168. [CrossRef]
6. Wang, Z.; Li, P.; Liu, H.; Yang, J.; Liu, S.; Xue, L. Objective sound quality evaluation for the vehicle interior noise based on responses of the basilar membrane in the human ear. *Appl. Acoust.* **2021**, *172*, 107619. [CrossRef]
7. Genuit, K.; Schutte-Fortkamp, B.; Fiebig, A. Acoustical comfort of vehicles: A combination of sound and vibration. *J. Acoust. Soc. Am.* **2005**, *118*, 1920. [CrossRef]
8. Kuznetsov, K.; Lavrov, V.; Moshkov, P.; Rubanovsky, V. Designing of RRJ-95NEW-100 aircraft with regard to cabin noise requirements. *Akustika* **2021**, *41*, 34–39. [CrossRef]
9. Haxter, S.; Spehr, C. Two-Dimensional Evaluation of Turbulent Boundary Layer Pressure Fluctuations at Cruise Flight Conditions. In Proceedings of the 18th AIAA/CEAS Aeroacoustics Conference, Colorado Springs, CO, USA, 4–6 June 2012; AIAA Paper No. 2012-2139; ARC: Reston, VA, USA, 2012. [CrossRef]
10. Klabes, A.; Herr, M.; Appel, C.; Bouhaj, M. Fuselage Excitation During Cruise Flight Conditions: Measurement and Prediction of Pressure Point Spectra. In Proceedings of the 21st AIAA/CEAS Aeroacoustics Conference, Dallas, TX, USA, 22–26 June 2015; AIAA Paper No. 2015-3115; ARC: Reston, VA, USA, 2015. [CrossRef]
11. Bassetti, A.; Guerin, S. Semi Empirical Jet Noise Modelling for Cabin Noise Predictions—Acoustic Loads in the Geometric Near Field. In Proceedings of the 17th AIAA/CEAS Aeroacoustics Conference, Portland, OR, USA, 5–8 June 2011; AIAA Paper No. 2011-2925; ARC: Reston, VA, USA, 2011. [CrossRef]
12. Samokhin, V.; Moshkov, P.; Yakovlev, A. Analytical model of engine fan noise. *Akustika* **2019**, *32*, 168–173. [CrossRef]
13. Baklanov, V.S. Role of structural noise in aircraft pressure cockpit from vibration action of new-generation engines. *Acoust. Phys.* **2016**, *62*, 456–461. [CrossRef]
14. Yan, X.; Sun, X.; Wang, D. Acoustics analysis and experimental study on silencer for commercial airplane air conditioning system. In Proceedings of the International Conference on Aerospace System Science and Engineering, Online, 14–16 July 2021; Springer Nature: Singapore, 2022; Volume 849, pp. 645–651. [CrossRef]
15. Golovasticova, A.V.; Vasilev, V.P.; Baklanov, V.S. Vibroacoustic characteristics of hydraulic system of the plane. *VDI Berichte* **2007**, *2002*, 589–594.
16. Moshkov, P. Experimental determination of wall pressure fluctuations on a Superjet 100 fuselage at level flight conditions. *Aerosp. Syst.* **2023**, *6*, 143–149. [CrossRef]
17. Alaoui, M.; Gloerfelt, X.; Collery, O.; Etchessahar, M. Effect of pressure gradients on turbulent boundary layer vortical structures and wall-pressure fluctuations. In Proceedings of the 21st AIAA/CEAS Aeroacoustics Conference, Dallas, TX, USA, 22–26 June 2015; AIAA Paper No. 2015-3116; ARC: Reston, VA, USA, 2015. [CrossRef]
18. Cohen, E.; Gloerfelt, X. Effect of pressure gradients on turbulent boundary layer noise and wall-pressure fluctuations. In Proceedings of the 21st AIAA/CEAS Aeroacoustics Conference, Dallas, TX, USA, 22–26 June 2015; AIAA Paper. No. 2015-3117; ARC: Reston, VA, USA, 2015. [CrossRef]
19. Haxter, S.; Spehr, C. Comparison of model predictions for coherence length to in-flight measurements at cruise conditions. *J. Sound Vib.* **2017**, *390*, 86–117. [CrossRef]
20. Robertson, J.E. *Prediction of In-Flight Fluctuating Pressure Environments Including Protuberance Induced Flow*; NASA CR 119947; NASA: Washington, DC, USA, 1971.
21. Cockburn, J.A.; Robertson, J.E. Vibration response of spacecraft shrouds to inflight fluctuating pressures. *J. Sound Vib.* **1974**, *33*, 399–425. [CrossRef]
22. Efimtsov, B.M. Characteristics of the field of turbulent wall pressure fluctuations at large Reynolds numbers. *Sov. Phys. Acoust.* **1982**, *28*, 289–292.

23. Efimtsov, B.M. Similarity criteria for the spectra of wall pressure fluctuations in a turbulent boundary layer. *Sov. Phys. Acoust.* **1984**, *30*, 33–35.

24. Rackl, R.; Weston, A. *Modeling of Turbulent Boundary Layer Surface Pressure Fluctuation Auto and Cross Spectra-Verification and Adjustments Based on TU-144LL Data*; NASA CR 2005-213938; NASA: Washington, DC, USA, 2005.

25. Moshkov, P. Contributions of Different Sources to Cabin Noise of a Superjet 100 in Cruise Flight Condition. In Proceedings of the 2021 AIAA Aviation Forum, Virtual Event, 2–6 August 2021; AIAA Paper No. 2021-2272; ARC: Reston, VA, USA, 2021. [CrossRef]

26. Abdrashitov, R.; Golubev, A. Identification of sources of noise in the cabin and the definition of the local passage of sound energy through fuselage based on the results of in-flight measurements of the Superjet. In Proceedings of the 21st AIAA/CEAS Aeroacoustics Conference, Dallas, TX, USA, 22–26 June 2015; AIAA Paper No. 2015-3114; ARC: Reston, VA, USA, 2015. [CrossRef]

27. Efimtsov, B.M.; Golubev, A.Y.; Kuznetsov, V.B.; Rizzi, S.A.; Andersson, A.O.; Rackl, R.G.; Andrianov, E.V. Effect of transducer flushness on measured surface pressure fluctuations in flight. In Proceedings of the 43rd AIAA Aerospace Sciences Meeting and Exhibit, Reno, NV, USA, 10–13 January 2005; AIAA Paper No. 2005-800; ARC: Reston, VA, USA, 2005. [CrossRef]

28. Hu, N.; Buchholz, H.; Herr, M.; Spehr, C.; Haxter, S. Contributions of Different Aeroacoustic Sources to Aircraft Cabin Noise. In Proceedings of the 19th AIAA/CEAS Aeroacoustics Conference, Berlin, Germany, 27–29 May 2013; AIAA Paper. No. 2013-2030. ARC: Reston, VA, USA, 2013. [CrossRef]

29. Lavrov, V.; Moshkov, P.; Popov, V.; Rubanovskiy, V. Study of the Sound Field Structure in the Cockpit of a Superjet 100. In Proceedings of the 25th AIAA/CEAS Aeroacoustics Conference (Aeroacoustics 2019), Delft, The Netherlands, 20–23 May 2019; AIAA Paper No. 2019-2726. ARC: Reston, VA, USA, 2019. [CrossRef]

30. Moshkov, P.A.; Strelets, D.Y. Problems of a Supersonic Business Aircraft Design with Regard to Cabin Noise Requirements. In *Recent Developments in High-Speed Transport*; Springer Aerospace Technology; Springer: Singapore, 2023; pp. 151–170. [CrossRef]

31. Moshkov, P.; Lavrov, V. Analysis of Vibroacoustics of the Superjet 100 Aircraft. In Proceedings of the 2022 International Conference on Dynamics and Vibroacoustics of Machines, Samara, Russia, 21–23 September 2022. [CrossRef]

32. Mabe, J.; Cabell, R.; Butler, G. Design and Control of a Morphing Chevron for Takeoff and Cruise Noise Reduction. In Proceedings of the 11th AIAA/CEAS Aeroacoustics Conference, Monterey, CA, USA, 23–25 May 2005; AIAA Paper No. 2005-2889; ARC: Reston, VA, USA, 2005. [CrossRef]

33. Mabe, J.; Calkins, F.; Butler, G. Boeing's Variable Geometry Chevron, Morphing Aerostructure for Jet Noise Reduction. In Proceedings of the 47th AIAA/ASME/ASCE/AHS/ASC Structures, Structural Dynamics, Newport, RI, USA, 1–4 May 2006; AIAA Paper No. 2006-2142; ARC: Reston, VA, USA, 2006. [CrossRef]

34. Mengle, V.; Ganz, U.; Bultemeier, E.; Calkins, F. Clocking Effect of Chevrons with Azimuthally-Varying Immersions on Shock-cell/Cabin Noise. In Proceedings of the 14th AIAA/CEAS Aeroacoustics Conference (29th AIAA Aeroacoustics Conference), Vancouver, BC, Canada, 5–7 May 2008; AIAA Paper No. 2008-3000; ARC: Reston, VA, USA, 2008. [CrossRef]

35. Vieira, A.; Koch, M.; Bertsch, L.; Snellen, M.; Simons, D.G. Simulation Methodologies of Engine Noise Shielding by Wings Within Conceptual Aircraft Design. *J. Aircr.* **2020**, *57*, 1202–1211. [CrossRef]

36. Vieira, A.; Snellen, M.; Simons, D.G. Assessing the shielding of engine noise by the wings for current aircraft using model predictions and measurements. *J. Acoust. Soc. Am.* **2018**, *143*, 388–398. [CrossRef]

37. Greco, G.F.; Bertsch, L.; Ring, T.P.; Langer, S.C. Sound quality assessment of a medium-range aircraft with enhanced fan-noise shielding design. *CEAS Aeronaut. J.* **2021**, *12*, 481–493. [CrossRef]